RSC Advances

ROYAL SOCIETY OF CHEMISTRY

www.rsc.org/advances

RSC Advances

ARTICLE

Allantoin-loaded porous silica nanoparticles / polycaprolacton nanofiber composites: fabrication, characterization, and drug release properties

Received 00th October 20xx,
Accepted 00th ---------- 20xx

DOI: 10.1039/x0xx00000x

www.rsc.org/

Ma Ke[a], Jatoi Abdul Wahab[a,b], Bang Hyunsik[a], Kyung-Hun Song[c], Jung Soon Lee[d], Mayakrishnan Gopiraman[a,*], Ick Soo Kim[a,*]

Development of biocompatible nanocomposites for biomedical applications such as drug release has attained greater attention in recent years. We report porous silica nanoparticles (PSNs) immobilized polycaprolacton (PCL) nanofiber composites (PCL/PSNs) for drug delivery applications. The allantoin (model drug) loaded PSNs were mixed well with PCL solution and electrospun to fabricate the PCL/PSNs nanofiber composites. The PSNs were prepared from rice husk, allantoin was loaded on PSNs to prepare (allantoin-PSNs), then its three different concentrations (10, 20 and 30 wt %) based on PCL wt.% were chosen. Biocompatibility and biodegradability of PCL, higher adsorption and nontoxicity of mesoporous silica nanoparticles and promising results of PCL/PSNs composite confer the system contesting potential for controlled drug delivery applications. The prepared PSNs, PCL nanofibers and PCL/Allantoin-PSNs nanofiber composites were characterized by scanning electron microscopy-energy dispersive spectroscopy (SEM-EDS), transmission electron microscopy (TEM), X-ray diffraction (XRD), X-ray photoelectron microscopy (XPS), Fourier transform infra-red spectroscopy (FTIR), and drug release analysis. The results confirmed the successfully synthesis of mesoporous nanoscopic PSNs from rice husk and controlled Allantion release profile by the resultant PCL/Allantoin-PSNs nanofiber composites.

1. Introduction

Nanotechnology has already revolutionized scientific world owing to the very small size and greater surface area of the unique nanoscopic materials. Since the historical breakthrough of nanotechnology and developments[1-5], numerous new application domains has been captured such as filters[6], wipes[7], drug delivery systems[8-9], battery and capacitor electrodes[10-11], regenerative scaffolds[12-13], biosensors[14] and catalysts[15]. Electrospinning has received greater recognition due to simplicity, versatility and diversity[16-19]. The electrospun polymer nanofibers and their composites have received greater attention and versatile exploitations in various applications.[19-21] Particularly, the heterogeneous porous nanoparticles (PNs) such as silica (PSNs) and alumina PNs immobilized nanofiber composites are reported as efficient candidates for biomedical applications due to their prominent characteristics and performance in comparison to traditional materials.[22-24, 16]

The PSNs have been exploited in drug delivery applications owing to their large surface area (greater than 700m^2/gram), high pore volume (greater than 0.9m^3/g), tunable nanoscopic pore size within narrow range of 2 to 10 nm and stability against thermal and chemical agents[22-24]. For an effective and viable drug delivery system, a drug carrier need to overcome four major problems such as loading and activated release capacity for large group of drugs, controlled release of therapeutics at their targeted location without premature discharge, nontoxicity and cost effectiveness. Vast availability of silica in nature, cost-effective and tailorable fabrication, tunable mesoporous structure, nontoxicity, biocompatibility and controllable adsorption/desorption profile along with greater specific surface area and pore size endow PSNs unique properties suitable for drug delivery applications[25]. Furthermore, tailored adsorption and release characteristics of the PSNs can be achieved by tuning its porous architecture, pore size and by surface functionalization[26-29]. These unique characteristics define wider PSN's applications ranging from biomedical [30-31], filtration [32], sensor [33] to imaging [32,34-37].

The surface of PSNs is largely composed of silanol groups (Si-OH) with weak acidic characteristics. Thanks to the existence of these silanol groups it can be easily modified with various silylating agents. For drug delivery applications, surface interaction between the drug and the host (PSNs) is primarily chemical interaction between free silanol groups of PSNs and functional groups in the drug molecules. For loading and unloading of the drug molecules, PSNs posses open entrances and ordered channels for entrance, homogenous distribution and release of drug molecules[37]. However, it is necessary to consider the functional interaction and molecular size vs. pore size between the to-be delivered drug and PSNs[25]; a drug with molecular size larger than pore size of PSN would not be a successful case.

On the other hand, PCL as a base polymer has been chosen owing to its vast applicability and characteristics suitable for biomedical applications. It is a semi-crystalline aliphatic polyester with lower Tg (-60°C) possessing broader in-vivo and in-vitro bio-

[a] Nano Fusion Technology Research Group, Department of Bioscience and Technology, Interdisciplinary Graduate School of Science and Technology, Shinshu University, Tokida, Ueda, Nagano Prefecture, 386-8567, Japan. E-mail addresses: kim@shinshu-u.ac.jp (I.S. Kim) and gopiramannitt@gmail.com (M. Gopiraman).
[b] Nanomaterials Research Lab., Department of Textile Engineering, Mehran University of Engineering and Technology, Jamshoro, Sindh, Pakistan
[c] Department of Clothing & Textiles, PaiChai University, Daejeon 302-735, South Korea
[d] Department of Clothing and Textiles, Chungnam National University, Daejeon 305-764, South Korea

Electronic Supplementary Information (ESI) available: SEM images and BET isotherm curves are provided. See DOI: 10.1039/x0xx00000x

compatibility. It has been reported to be biocompatible and bio-resorbable for both soft and hard tissues [38-39]. U.S. Food and Drug Administration has approved PCL for substantial number of drug delivery and other biomedical applications [40].

In this research, the PSNs were synthesized from rice husk. Although several other methods of PSNs preparation are available, however, a new method for PSNs preparation from rice husk has been developed. This technique of PSNs preparation from rice husk bestow twofold advantages such as environmental problems of rice husk disposal and pollution could be solved along with effective utilization of an extensively available natural resource. Since burning rice husk in air produces large quantity of environmental pollutants such as CO_2, SO_x and NO_x and its untreated discarding results airborne breathing problems due to its low density [41-42]. The second advantage of silica nanoscopic particle synthesis from rice husk is the preparation cost which is very low in comparison to its highly sophisticated applications [43].

Although sufficient work has been done on nanoporous silica particles and PCL, however, very little literature is available on PSNs synthesis from rice husk and it's composite with PCL as drug carrier. Therefore our study on electrospun nanocomposite mat composed of PCL/PSNs loaded with allantoin (Fig. 1) as guest drug is reported. For optimization three concentrations (wt. %) of allantoin loaded PSNs (10%, 20% and 30%) were used. The results obtained by characterization with SEM, TEM, XRD, XPS, EDS, FTIR and drug release analysis confirm the composite mat as suitable and controlled allantoin release nanocomposite mat for biomedical applications with tunable release profile.

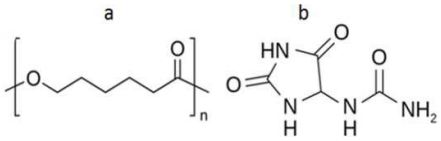

Fig. 1 Chemical structure of PCL (a) allantoin (b)

Owing to excellent biocompatibility and nontoxicity of PCL, nontoxicity of mesoporous PSNs, the PCL/PSNs nanocomposite can be considered as a nontoxic and viable drug carrier medium. Thus it can be suitably exploited in drug delivery systems, tissue engineering and other biomedical applications. Further research on PCL/PSNs nanocomposite may further unfold its candidacy for biomedical applications.

2. Experimental

2.1 Materials

Polycaprolactone (PCL, Mn: 70,000–90,000), dichloromethane (DCM), allantoin, hydrochloric acid (HCl), phosphate buffer powder (PBS, 1/15 mol/L with pH 7.2), and dimethylformamide (DMF) were purchased from Sigma-Aldrich or Wako Pure Chemicals. All chemicals were used without further purification. Rice husks were collected from Aichi Prefecture of Japan, and processed before use.

2.2 Preparation of PSNs

The rice husk (500 g) was washed and dried at 60°C for 24 h in order to remove the potassium, calcium and other metal components. The rice husk contains 55-60 wt.% of cellulose and about 22 wt.% of lignin out of its organic constituents [43]. In order to remove these constituents, a 50 g of the dried husk was stirred in 0.1 M HCl (500 ml) at 27°C for 24 h. Then, the husk was calcinated in a muffle furnace at 600°C at 10°C/min. The resultant powder was crushed by using a mortar to produce fine silica particles. Subsequently, the crushed porous silica particles were dispersed in distilled water and kept for 1 h. Finally, by complete removal and evaporation of water, PSNs were obtained.

2.3 Loading of allantoin on PSNs

The equal weights of allantoin and PSNs (0.3 g each) were added in 500 ml of water. The solution was stirred for 6 h under dark condition. Then the PSNs were separated by centrifugal separator (XX42CFO RT, Nihon Millipore K.K, Japan) at 6200 rpm. To remove loosely held allantoin, the drug loaded PSNs were stirred in distilled water and processed in the centrifugal separator. The drug loaded silica nanoparticles were finally dried to remove water and used to fabricate the PCL-composites.

2.4 PCL/PSNs solution preparation

Dichloromethane (DCM) and dimethyl formamide (DMF) in three w/w ratios 8:2, 6:4 and 4:6 respectively, were used as solvent for polycaprolactone (PCL). Three different PCL concentrations (8%, 10% and 12% by weight) were mixed with each solvent formulation for optimal electrospinning solution. It was experimentally observed from the results (Figs. S1, S2 and S3) that 10% PCL concentration and 6:4 DCM: DMF ratio produced smooth and regular PCL nanofiber without beads in the structure along with lower mean diameter. Lower diameter of nanofibers allows higher permeability [44] for liquids along with increased specific surface area which enhances adhesion among the fibers. In the other PCL and solvents formulations undesirable results (beads, ruptures, surface and structural irregularities) were observed. Hence, 10% PCL concentration and 6:4 DCM: DMF was used for further experimentation and PCL/PSNs nanofiber composite formation. Subsequently, three allantoin containing silica particle concentrations (10, 20 and 30 wt %) were added into the PCL solution. The PCL/allantoin-PSNs solution was then stirred for 12 h in order to obtain a homogeneous solution.

2.5 Electrospinning process

For electrospinning, Har-100*12, Matsusada Co., Tokyo, Japan, electrospinning apparatus with grounded rotary drum collector covered with aluminium foil was used. The applied voltage was 10kV and needle tip to collector distance was 15 cm.

2.6 Drug release test

The drug releases characteristics of the prepared samples were investigated by immersing the nanofibers composites into a 50 mL of PBS (pH 7.2) and thermostatically shaking (100 rpm) at 36°C for 5 days. For determination of drug concentration, 4 ml of the test solution was taken at particular time intervals, then for capacity adjustment, a 4 ml of new test solution was added. After drug release test, the samples were vacuum dried for 24 hours. UV-visible spectrophotometer (V-530, JASCO, Japan) was used to determine concentration of the released allantoin from collected test solution. For determining the concentration of allantoin, a

calibration curve by ultraviolet-visible absorption spectrum of allantoin was prepared in advance.

2.7 Characterization

The morphological of the electrospun mats was investigated with SEM-EDS (Hitachi 3000H SEM). For morphological study of nanofibers and silica nanoparticles FE-SEM (S-5000, Hitachi Co., Japan) and TEM (JEOL model 2010 Fas TEM) were used. The X-ray photoelectron spectrometer (KratosAxis-Ultra DLD, Kratos Analytical Ltd, Japan) and EDS measurements were performed to confirm elemental composition of the silica. FTIR analysis (IR Prestige-21, Shimadzu, Japan) was carried out in order to study chemical structure of surface of the porous silica particles. The specific surface area of samples was determined using the Brunauer-Emmett-Teller (BET) method (BELSORP-max, BEL Japan, Inc.). In addition, test temperature was maintained at 36 ℃ by using thermostat (SLI-200, EYELA, Japan), during drug release test the tested sample was immersed in the test solution by using shaker (NX-20, NISSIN, Japan) under 100 rpm.

3. Results and Discussion

3.1 Characterization of rice husk and PSNs

After HCL treatment the color of rice husk changed to paler and lighter in comparison to its darker colored precursor, which confirms the removal of the impurities from rice husk such as lignin, cellulose and others (Fig. S4). The macro structure of the husk and porous silica (Fig. 2a & 2b) shows their uneven surface. The PSNs surface can be observed with lower crests and falls in comparison to its precursor. The smoother surface of the husk (Fig. 2c) and porous structure of silica (Fig. 2d) confirms formation of fine pore in the later. The magnified SEM images of PSNs (Fig. 2f) further confirm its porous structure.

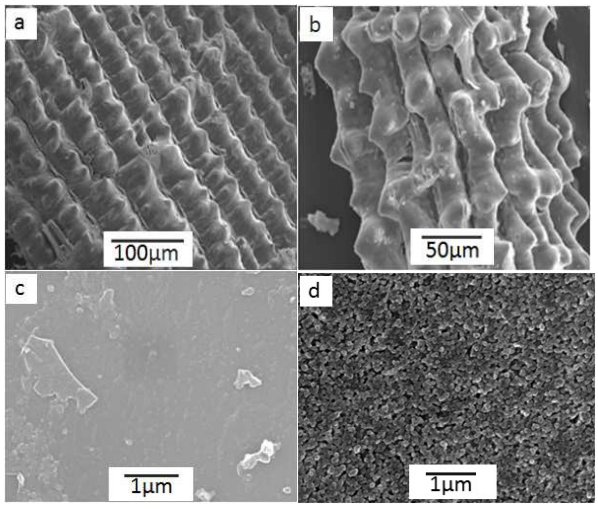

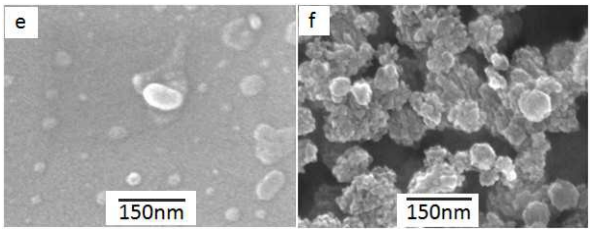

Fig. 2 SEM images of rice husk (a, c, e) and PSNs (b, d, f)

3.1.2 XPS and EDS analyses

The surface of PSNs is largely contains silanol groups (Si-OH) while the rice husk constitutes of organic materials along with some minerals. These chemical constituents in both are confirmed in the XPS and EDS spectra in Fig. 3 and Fig. 4 respectively. The XPS spectra for porous silica (Fig. 3a) show peaks of O 1s, Si 2p and Si 2s at 530 eV, 100eV and 145 eV respectively, while, for husk (Fig. 3b) shows peaks of C 1s and K 2s at 280 eV and 400 eV respectively. The absence of C 1s and K 2s peaks in PSNs confirms the removal of potassium and organic ingredients. The EDS results (Fig. 4) further confirm reduction of carbon and increase of silicon and oxygen.

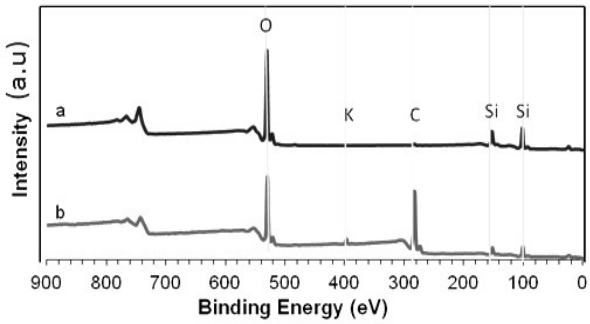

Fig. 3 XPS spectra for rice husk (a) PSNs (b)

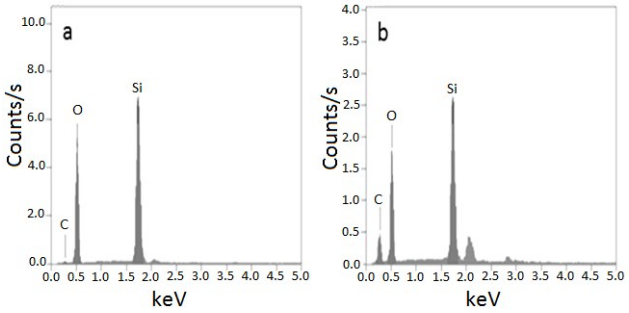

Fig. 4 EDS spectra of porous silica (a) rice husk (b)

3.1.3 FTIR analysis

The distinct features of PSNs are its internal structure composed of Si-O-Si with silanol group (Si-OH) at its surface (Fig. S5). FTIR results (Fig. 5) for PSNs and rice husk show respective peaks. The peaks at 1027 cm^{-1} and 793 cm^{-1} prove the existence of Si-O-Si. The peaks of organic components at 3000-2870 cm^{-1} and at 1430-1250 cm^{-1} present in rice husk (Fig. 5b) disappear in spectrum of porous silica (Fig. 5a) which confirms removal of organic components. At nearly 945 cm^{-1}, we can see shoulder peak of Si-O-Si. These products were

from Si-OH which indicates presence of Si-OH on the surface of porous silica and the internal structure composed of Si-O-Si.

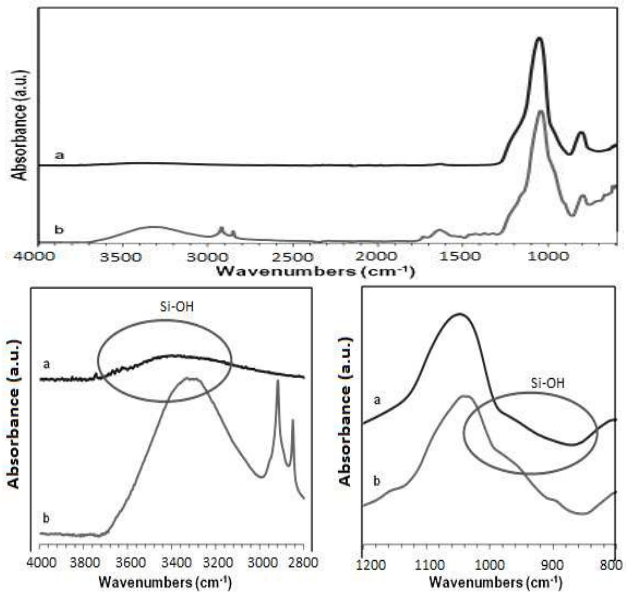

Fig. 5 FTIR spectra of PSNs (a) rice husk (b) demonstrating enlarged Si-OH peaks in the two figures at bottom

3.1.4 XRD analysis

The crystalline silica (Group 1) is carcinogenic for human, while, non-crystalline silica (Group 2) is non-carcinogenic and safe for human life. The Group 2 silica, owing to its biocompatibility is widely used as additive in medical applications. The XRD result of porous silica prepared in this experiment (Fig. 6) show a gentle peak at 2Θ = 22.5 ° which prove it to be non-crystalline [45] and thus safe for human body [36].

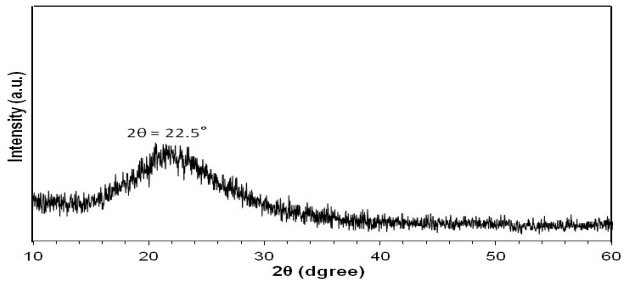

Fig. 6 XRD spectra of porous silica

3.2 Porous silica nanoparticles

3.2.1 TEM analysis

In the TEM images of silica nanoparticles (Fig. 7), voids derived from fine pores in the particles can be seen which confirms presence of fine pores in the pulverized porous silica. The particle size distribution of silica nanoparticles obtained through light dynamic scattering method is described in Fig. 8. The pulverized porous silica solution without a supernatant (Fig. 8b) contains coarser particle while where the supernatant was added after three hours (Fig. 8a) contains fine particles with average diameter of 220 nm and polydispersity index (PDI) of 0.221. The particles were uniformly dispersed (monodisperse).

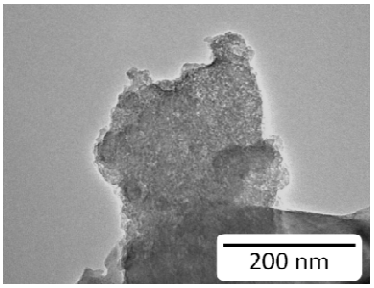

Fig. 7 TEM image of porous silica nano particles

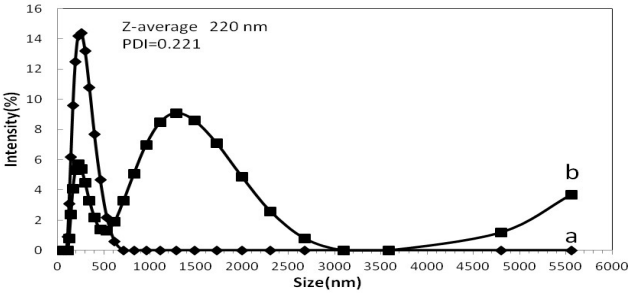

Fig. 8 Particle size distribution of PSNs when supernatant added after 3 (a) and PSNs dispersion without supernatant (b)

3.2.2 Analysis of pore characteristics

The surface area and pore size of PSNs can be measured by nitrogen gas adsorption-desorption isotherm method (BET method). From the nitrogen gas adsorption and desorption isotherms measured by the automatic specific surface area measuring device the specific surface area was found to be 334 m^2/g and average pore size of 3.57nm proving that the porous silica is mesoporous.

Considering the previous FE-SEM image (Fig. 2), pores with pore size from several nanometers to several tens of nanometers can be observed. Combining FE-SEM image (Fig. 2) and the nitrogen gag adsorption-desorption results (Fig.9 & Fig.10), it was clear that not only the surface but also the internal parts of porous silica had a porous structure. The results indicated tubular pore shape and uniform porous structure of PSNs.

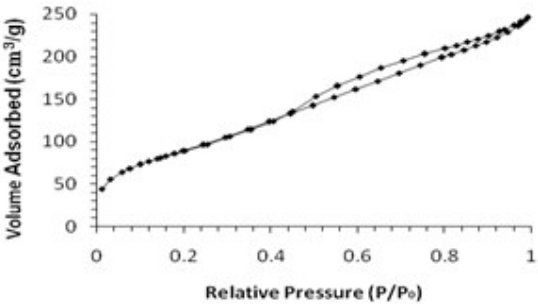

Fig. 9 Nitrogen adsorption–desorption isotherm

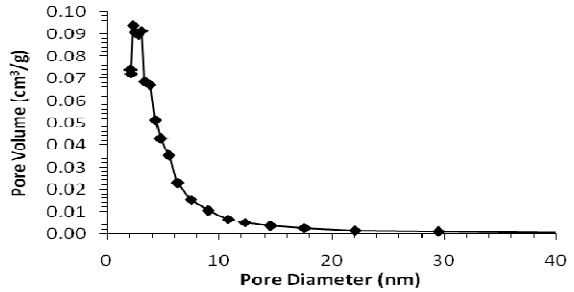

Fig. 10 The BJH porous distribution

3.3 PCL/PSNs nanofiber composite

3.3.1 SEM and TEM analyses

With the incorporation and subsequent addition of PSNs with PCL to form PCL/allantoin-PSNs nanofiber composite, nanofiber diameter of the composite increased and cobb-like projections were observed (Fig. 11). The TEM images (Fig. 12) show PSNs enveloped inside the PCL nanofibers which also confirm aggregation of the porous structure. Cobb-like projections of the silica particles at the surface of nanofiber structure are also observed in the PCL/ allantoin-PSNs composite.

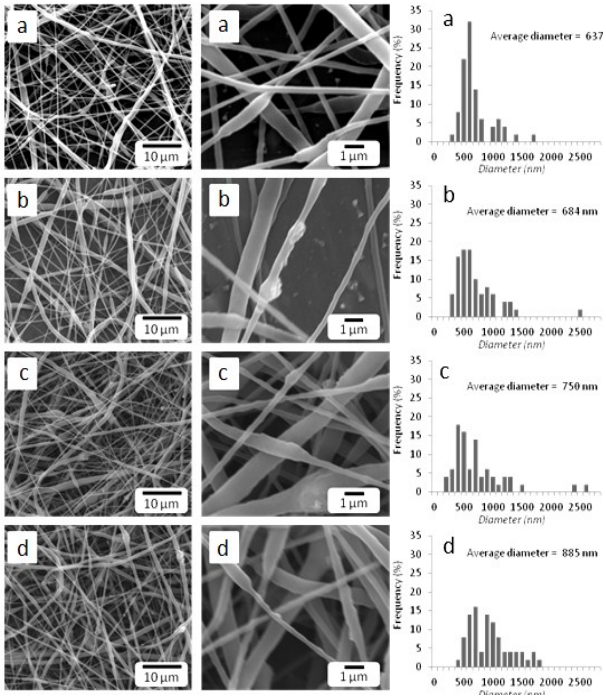

Fig. 11 SEM images and diameter distribution of PCL/allantoin-PSNs nanofiber composite with PSNs with 0 wt% **(a)** 10 wt% **(b)** 20 wt% **(c)** 30 wt% **(d)**.

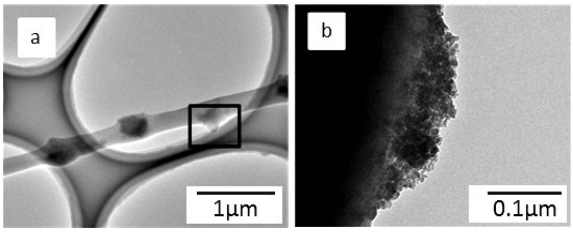

Fig. 12 TEM images of PCL/allantoin-PSNs nanofiber composite, PSNs enveloped in the nanofibers **(a)** cobb-like projections of PSNs **(b).**

3.3.2 FTIR evaluations of PCL/PSNs and PCL/allantoin-PSNs

The FTIR spectra of PCL/PSNs and PCL/allantoin-PSNs are described in Fig. 13. For all samples, the characteristic peaks of PSNs[46] can be observed at 1110cm^{-1}, 2850cm^{-1} and 2925cm^{-1}. In addition, PCL characteristic peaks[47] can be observed at 720cm^{-1}, 850-1480 cm^{-1} and at 1725 cm^{-1}. In case of PCL/allantoin-PSNs, the characteristic peaks of allantoin overlapped completely with the absorption bands of PCL and PSNs so that these bands are not available for the differentiation.

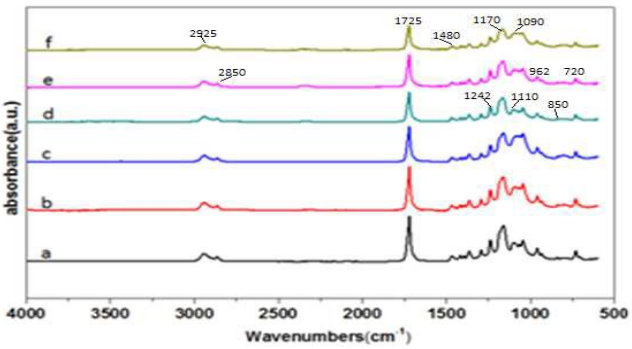

Fig. 13 FTIR spectrum of PCL/allantoin-PSNs 10% (a) 20% (b) 30%(c) and PCL/PSNs 10% (d) 20% (e) 30% (f)

3.3.3 Allantoin release analysis

The cumulative allantoin release from PSNs reached equilibrium state in about one hour (Fig. 14). The allantoin release results from the PCL/allantoin-PSNs nanocomposite are given in Fig. 15.

For pure PCL nanofibers rapid allantoin release can be observed in first 10 hours which then slows down resulting 80% released after 120 hours. Comparative higher allantoin release rate may be attributed to allantoin adsorption on the surface of PCL nanofibers and since allantoin is a polar molecule and has high affinity for DMF while the PCL and DMF have low affinity with each other. As a result, during the electrospinning process, the DMF concentration of PCL solution changed on volatilization and allantoin moves to the PCL nanofiber surface. Thus a rapid release of allantoin is observed at the beginning. A sustained releasing agent will help to obtain a sustained release of the drug that function is successfully accomplished *via* PSNs in this study.

The presence of PSNs in the PCL/allantoin-PSNs composite nanofibers may be considered as a sustained releasing agent. As the allantoin release in the first 10 hours of the process show 20%, 15% and 5% release with allantoin loaded PSNs of 30wt%, 20wt% and 15wt% respectively. The sustained release of allantoin by incorporation of PSNs may be attributed to the Si-OH functional groups and polarity of Si-O-Si bond in its structure. These groups prevented migration of allantoin onto the surface of PCL nanofibers during electrospinning of the composite. However, the increased release of allantoin with further addition of PSNs (20% and 30%) are probably the result of their increased density and projection outside of the nanofiber surface as confirmed by SEM and TEM images (Fig. 11 and 12).

Further evaluation of the results show that for first 30 hours of the process, PCL nanofibers without the PSNs released more than 60% of allantoin while for PCL/PSNs composite nanofibers released less than 30% with prominently lower release rate by 10% silica nanoparticles. The results confirm excellent performance of PCL/PSNs nanofiber composite for medical application such as wound healing with possibility to tailor the release rate *via* controlling the silica contents, hence, size and area of silica nanoparticles in the composite. Thus compilation of the results of current study encapsulates successful synthesis of PCL/allantoin-PSNs nanofiber composite for sustained drug release. Some of the work done by other researchers is further discussed below.

Yuvakkumar *et al*. [48] synthesized porous silica nanoparticles from rice husk by alkali (NaOH) extraction and following acidic extraction. The researchers claimed higher purity of silica by using 0.5 N, 1N, 1.5N, 2N and 2.5N NaOH with highest purity by 2.5N NaOH. They claimed preparation of silica nanoparticles with ~25 mean size, specific surface area of 274m^2/g and 1.46nm pore size. The research does not report further study for suitability of the nanoparticles for biomedical application such as drug delivery.

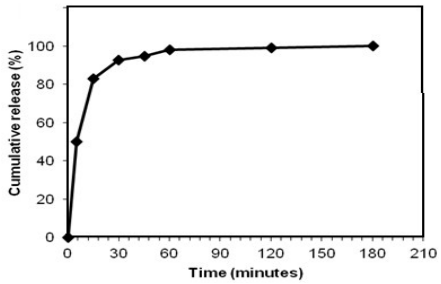

Fig. 14 Cumulative allantoin release from PSNs

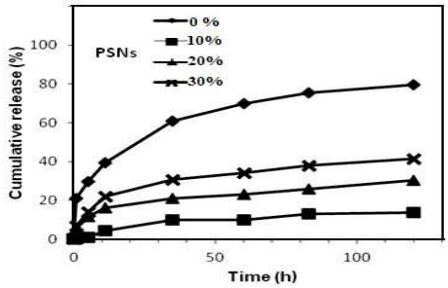

Fig. 15 Cumulative allantoin release from PCL/allantoin-PSNs nanofiber composite

In another study Hu *et al*. [48] successfully synthesized silica nanoparticles (nonporous) from rice straw using potassium silicate (KOH filtrate) by precipitation with polyethylene oxide (acidified) followed by calcinations at 500 °C for purification. The research prepared nonporous spherical silica nanoparticles with 100 to 120 nm particle size. The research did not report any extension for further study on application of these silica nanoparticles. Ahmed et el.[49] reported successful synthesis of silica micro and macro particles from miscanthus crop, cereal residues (pellets) and wheat straw. The biomass was thermo-chemically treated to produce the silica particles. The biomass was leached with H_2SO_4 (5M) followed by thermal treatment in muffle furnace. The research claimed highest silica content and specific surface area of 245 m^2/g from cereal pellets. The research does not further discuss the application and suitability of the meso and macro silica particles for biomedical applications. Kashanian *et al*.[50] discussed fabricated mesoporous silicon (pSi) encapsulated in biodegradable PCL microfibers via electrospinning to produce a nonwoven pSi/PCL mat for biomedical applications. The result of the study evinced successful encapsulation of pSi in the PCL microfibers by electrospinning and further disclosed biocompatibility of the mat with epithelial cells of rats. The study suggested possibility of controlled release kinetics via modifying Si surface. Sigh *et al*.[51] successfully prepared a multilayered mesoporous silica and PCL based nanoscopic biomatrix for bone regeneration and controlled loading and release capacity of the guest molecules. The polycaprolactone nanofibers were electrospun and coated with mesoporous silica by sol-gel technique. The mesoporous silica coating improved wetting, ionic reactivity and mechanical characteristics of the composite for bone regeneration. It was also disclosed that the mesoporous surface allowed capability for loading of proteins and drug molecules along with sustained drug release profile over extended time period. Although a little work is available for silica synthesis from different biomasses and agricultural waste, however, the method of synthesis of mesoporous silica nanoparticles from rice husk extends a wider domain of research for efficient and useful utilization of natural resources and synthesizing from them highly sophisticated materials for safety and survival of human life on the planet.

4. Conclusions

Results of the current study conclude a successful method of PSNs synthesis from rice husk resulting suitable utilization of natural resource along with mitigation of ecological problems from its untreated dumping in environment. The prepared PSNs, loaded with allantoin as sample drug, were successfully fabricated with PCL to produce PCL/PSNs nanofiber composite for sustained drug release. The guest loaded PSNs were added in three wt% concentrations with PCL (10%, 20% and 30%) subsequently electrospun into composite mat. The results reveal 10% PSNs in the composite producing slower release rate which subsequently increased with further addition of PSNs. Thus, it is confirmed from the results that by tuning PSN wt% in PCL/PSNs nanofiber composite controlled drug release profile can be achieved. Thus confirms PCL/PSNs composite as a sustained drug delivery nanofiber mat.

References

(1) Formalas, A. *J. Electrost* **1995**, *35*, 151.
(2) Doshi, J.; Reneker, D. H. In *Industry Applications Society Annual Meeting, 1993., Conference Record of the 1993 IEEE*; IEEE: 1993, p 1698.
(3) Shin, Y.; Hohman, M.; Brenner, M.; Rutledge, G. *Applied physics letters* **2001**, *78*, 1149.
(4) Reneker, D. H.; Yarin, A. L.; Fong, H.; Koombhongse, S. *Journal of Applied physics* **2000**, *87*, 4531.
(5) Fridrikh, S. V.; Jian, H. Y.; Brenner, M. P.; Rutledge, G. C. *Physical review letters* **2003**, *90*, 144502.
(6) Qin, X. H.; Wang, S. Y. *Journal of Applied Polymer Science* **2006**, *102*, 1285.
(7) Sudo, T.; Yamabe, T.; Kim, I. S.; Enomoto, Y. *Tribology Online* **2010**, *5*, 262.

(8) Yoo, H. S.; Kim, T. G.; Park, T. G. *Advanced drug delivery reviews* **2009**, *61*, 1033.
(9) Kenawy, E.-R.; Abdel-Hay, F. I.; El-Newehy, M. H.; Wnek, G. E. *Materials Chemistry and Physics* **2009**, *113*, 296.
(10) Kim, B.-H.; Yang, K. S.; Woo, H.-G. *Electrochemistry Communications* **2011**, *13*, 1042.
(11) Kim, C.; Yang, K. S.; Kojima, M.; Yoshida, K.; Kim, Y. J.; Kim, Y. A.; Endo, M. *Advanced Functional Materials* **2006**, *16*, 2393.
(12) Yoshimoto, H.; Shin, Y.; Terai, H.; Vacanti, J. *Biomaterials* **2003**, *24*, 2077.
(13) Kim, G.; Kim, W. *Journal of Biomedical Materials Research Part B: Applied Biomaterials* **2007**, *81*, 104.
(14) Baker, S. E.; Tse, K.-Y.; Lee, C.-S.; Hamers, R. J. *Diamond and related materials* **2006**, *15*, 433.
(15) Zhao, T.-J.; Sun, W.-Z.; Gu, X.-Y.; Rønning, M.; Chen, D.; Dai, Y.-C.; Yuan, W.-K.; Holmen, A. *Applied Catalysis A: General* **2007**, *323*, 135.
(16) Kim, H.-R.; Fujimori, K.; Kim, B.-S.; Kim, I.-S. *Composites science and technology* **2012**, *72*, 1233.
(17) Hu, X.; Liu, S.; Zhou, G.; Huang, Y.; Xie, Z.; Jing, X. *Journal of Controlled Release* **2014**, *185*, 12.
(18) Hernández, M. S.; Hernández, C. S.; Fuentes, A. G.; Elorza, E.; Carrera-Rodríguez, M.; Alquiza, M. J. P. *Journal of Sol-Gel Science and Technology* **2014**, *71*, 514.
(19) Bang, H.; Gopiraman, M.; Kim, B.-S.; Kim, S.-H.; Kim, I.-S. *Colloids and Surfaces A: Physicochemical and Engineering Aspects* **2012**, *409*, 112.
(20) Hou, H.; Ge, J. J.; Zeng, J.; Li, Q.; Reneker, D. H.; Greiner, A.; Cheng, S. Z. *Chemistry of Materials* **2005**, *17*, 967.
(21) Saeed, K.; Park, S.-Y.; Lee, H.-J.; Baek, J.-B.; Huh, W.-S. *Polymer* **2006**, *47*, 8019.
(22) Zhang, Q.; Wang, X.; Li, P. Z.; Nguyen, K. T.; Wang, X. J.; Luo, Z.; Zhang, H.; Tan, N. S.; Zhao, Y. *Advanced Functional Materials* **2014**, *24*, 2450.
(23) Song, B.; Wu, C.; Chang, J. *Acta biomaterialia* **2012**, *8*, 1901.
(24) Shadjou, N.; Hasanzadeh, M. *Journal of Biomedical Materials Research Part A* **2015**.
(25) Tang, F.; Li, L.; Chen, D. *Advanced Materials* **2012**, *24*, 1504.
(26) Alberti, S.; Soler-Illia, G. J.; Azzaroni, O. *Chemical Communications* **2015**, *51*, 6050.
(27) DeMuth, P.; Hurley, M.; Wu, C.; Galanie, S.; Zachariah, M. R.; DeShong, P. *Microporous and Mesoporous Materials* **2011**, *141*, 128.
(28) Wu, S.-H.; Hung, Y.; Mou, C.-Y. *Chemical Communications* **2011**, *47*, 9972.
(29) Thavasi, V.; Singh, G.; Ramakrishna, S. *Energy & Environmental Science* **2008**, *1*, 205.
(30) Liu, J.; Detrembleur, C.; Mornet, S.; Jérôme, C.; Duguet, E. *Journal of Materials Chemistry B* **2015**, *3*, 6117.
(31) Lu, X.; Wang, C.; Wei, Y. *Small* **2009**, *5*, 2349.
(32) Li, R.; Zhang, L.; Wang, P. *Nanoscale* **2015**.
(33) Walcarius, A. *Chemical Society Reviews* **2013**, *42*, 4098.
(34) Caltagirone, C.; Bettoschi, A.; Garau, A.; Montis, R. *Chemical Society Reviews* **2015**.
(35) Trewyn, B. G.; Nieweg, J. A.; Zhao, Y.; Lin, V. S.-Y. *Chemical Engineering Journal* **2008**, *137*, 23.
(36) Ukmar, T.; Planinšek, O. *Acta pharmaceutica* **2010**, *60*, 373.
(37) Slowing, I. I.; Vivero-Escoto, J. L.; Wu, C.-W.; Lin, V. S.-Y. *Advanced drug delivery reviews* **2008**, *60*, 1278.
(38) Hutmacher, D. W.; Schantz, T.; Zein, I.; Ng, K. W.; Teoh, S. H.; Tan, K. C. *Journal of Biomedical Materials Research* **2001**, *55*, 203.
(39) Pitt, C. G.; Chasalow, F.; Hibionada, Y.; Klimas, D.; Schindler, A. *Journal of applied polymer science* **1981**, *26*, 3779.
(40) Domb, A. J.; Kost, J.; Wiseman, D. *Handbook of biodegradable polymers*; CRC Press, 1998; Vol. 7.
(41) Chungsangunsit, T.; Gheewala, S. H.; Patumsawad, S. *World Acad. of Sci.: Eng. and Tech* **2009**, *53*, 1070.
(42) Bansal, V.; Ahmad, A.; Sastry, M. *Journal of the American Chemical Society* **2006**, *128*, 14059.
(43) Liou, T.-H. *Materials Science and Engineering: A* **2004**, *364*, 313.
(44) Ahn, J.; Chung, W.-J.; Pinnau, I.; Guiver, M. D. *Journal of membrane science* **2008**, *314*, 123.
(45) Jung, D. S.; Ryou, M.-H.; Sung, Y. J.; Park, S. B.; Choi, J. W. *Proceedings of the National Academy of Sciences* **2013**, *110*, 12229.
(46) Knežević, N. Ž.; Milenković, S.; Jović, D.; Lazarevic, S.; Mrdjanović, J.; Djordjevic, A. *Advances in Materials Science and Engineering* **2015**, *2015*.
(47) Wu, C.-S. *Polymer Degradation and Stability* **2003**, *80*, 127.
(48) Yuvakkumar, R.; Elango, V.; Rajendran, V.; Kannan, N. *Journal of Experimental Nanoscience* **2014**, *9*, 272.
(49) Ahmad Alyosef, H.; Schneider, D.; Wassersleben, S.; Roggendorf, H.; Weiß, M.; Eilert, A.; Denecke, R.; Hartmann, I.; Enke, D. *ACS Sustainable Chemistry & Engineering* **2015**, *3*, 2012.
(50) Kashanian, S.; Harding, F.; Irani, Y.; Klebe, S.; Marshall, K.; Loni, A.; Canham, L.; Fan, D.; Williams, K. A.; Voelcker, N. H. *Acta biomaterialia* **2010**, *6*, 3566.
(51) Singh, R. K.; Jin, G.-Z.; Mahapatra, C.; Patel, K. D.; Chrzanowski, W.; Kim, H.-W. *ACS applied materials & interfaces* **2015**, *7*, 8088.

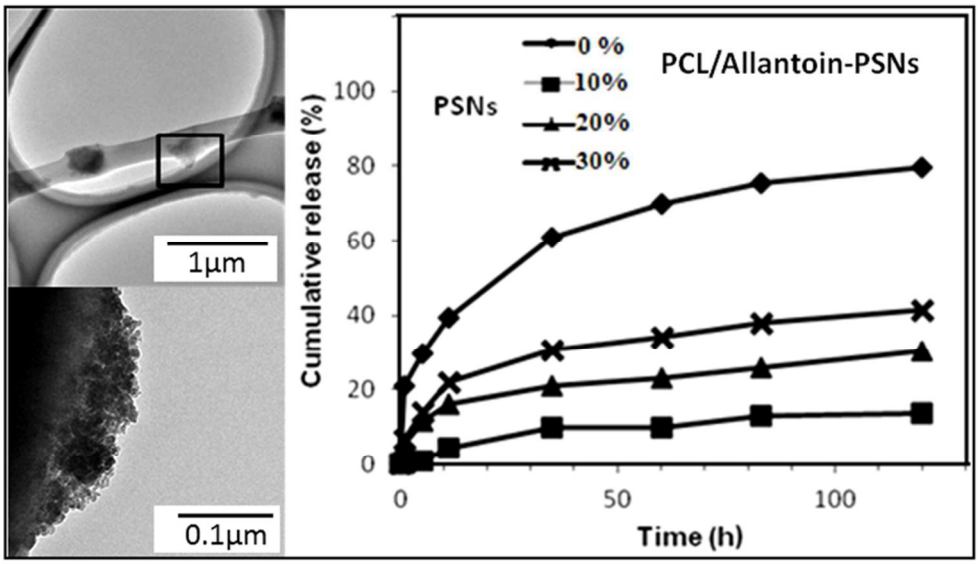

254x190mm (96 x 96 DPI)